Aviation-induced radiative forcing and surface temperature change in dependency of the emission altitude

C. Frömming,[1] M. Ponater,[1] K. Dahlmann,[1] V. Grewe,[1] D. S. Lee,[2] and R. Sausen[1]

Received 31 May 2012; revised 8 August 2012; accepted 28 August 2012; published 3 October 2012.

[1] The present study provides a detailed assessment of the net impact of global flight altitude changes on radiative forcing and temperature response. Changes in contrail coverage, chemical perturbations (H_2O, O_3, CH_4) and associated radiative forcings were determined from simulations with a quasi CTM. Future development of global mean radiative forcing and temperature response was calculated by means of a linear response model. The range of possible effects arising from various future scenarios is analyzed, and tradeoffs between partially counteracting short- and long term effects are studied. Present-day global mean radiative forcing of short-lived species and CH_4 is reduced when flying lower, whereas that of CO_2 increases. The opposite effect is found for higher flight altitudes. For increasing and sustained emissions, the climate impact changes are dominated by the effect of short-lived species, yielding a reduction for lower flight altitudes and an increase for higher flight altitudes. For future scenarios involving a reduction or termination of emissions, radiative forcing of short-lived species decreases immediately, that of longer lived species decreases gradually, and respective temperature responses start to decay slowly. After disappearance of the shorter lived effects, only the counteracting CO_2 effect remains, resulting in an increased climate effect for lower flight altitudes and a decrease for higher flight altitudes. Incorporating knowledge about the altitude sensitivity of aviation climate impact in the route planning process offers substantial mitigation potential. Scenarios and time horizons for the evaluation of future effects of mitigation instruments must be chosen carefully depending on the mitigation aim.

Citation: Frömming, C., M. Ponater, K. Dahlmann, V. Grewe, D. S. Lee, and R. Sausen (2012), Aviation-induced radiative forcing and surface temperature change in dependency of the emission altitude, *J. Geophys. Res.*, *117*, D19104, doi:10.1029/2012JD018204.

1. Introduction

[2] The effects of non-CO_2 aircraft emissions on the chemical composition of the atmosphere and on aviation-induced cloudiness are highly dependent on chemical and meteorological background conditions, thus they vary significantly with geographic location, altitude, and time of the emission. Considering such knowledge about altitude and location dependencies of air traffic effects in the route-planning process could potentially reduce the aviation net climate impact. The altitudinal dependency of contrails, aviation H_2O and NO_x effects has been investigated in several previous studies [e.g., *Sausen et al.*, 1998; *Grewe et al.*, 2002b; *Fichter et al.*, 2005; *Gauss et al.*, 2006; *Köhler et al.*, 2008; *Rädel and Shine*, 2008], which identified a number of characteristic sensitivities to emission altitudes and crucial inherent tradeoffs between warming and cooling contributions and between short-term and long-term effects.

[3] The potential of contrail mitigation has been addressed by shifting air traffic cruise altitudes globally toward higher or lower altitudes [*Sausen et al.*, 1998; *Fichter et al.*, 2005], or by restricting cruise altitudes over certain regions on a monthly basis [e.g. *Williams et al.*, 2002]. Another approach has been the investigation of small changes in flight altitude, depending on actual meteorological conditions, to avoid flying in ice supersaturated regions [*Mannstein et al.*, 2005]. All studies found a substantial contrail avoidance potential and evidence of regionally and seasonally compensating effects. While the present paper focuses on the climate impact of general flight altitude changes, the relation to an approach of route optimization adapted to actual weather situations will also be discussed.

[4] The water vapor increase induced by aviation depends on altitude, as has been found by *Gauss et al.* [2003] who studied the effect from water vapor emissions from cryoplanes. Higher flight altitudes lead to a larger fraction of water vapor emitted in the stratosphere, where water vapor

[1]Institut für Physik der Atmosphäre, Deutsches Zentrum für Luft- und Raumfahrt, Oberpfaffenhofen, Germany.
[2]Dalton Research Institute, Manchester Metropolitan University, Manchester, UK.

Corresponding author: C. Frömming, Institut für Physik der Atmosphäre, Deutsches Zentrum für Luft- und Raumfahrt, Oberpfaffenhofen, DE-82234 Wessling, Germany. (christine.froemming@dlr.de)

0148-0227/12/2012JD018204

Table 1. Annual Mean Flown Distance, Fuel Consumption and NO_x Emission for the TRADEOFF 2000 Base Case and the Flight Altitude Change Scenarios

Scenario	Flown Distance (10^9 km/yr)	Fuel Consumption (Tg/yr)	NO_x Emission (Tg(N)/yr)
+2000 ft	25.4	151	0.61
Base case	25.4	152	0.60
−2000 ft	25.4	156	0.62
−4000 ft	25.4	160	0.63
−6000 ft	25.4	161	0.63

emissions accumulate to larger concentration changes due to the lack of major loss processes.

[5] Changes in O_3 and CH_4 resulting from air traffic NO_x emissions are also highly dependent on the emission altitude. Air traffic-induced O_3 perturbations were found to increase for higher cruise altitudes and decrease for lower cruise altitudes [*Grewe et al.*, 2002b; *Gauss et al.*, 2006; *Köhler et al.*, 2008]. The reduced ozone impact for lower flight altitudes is mainly caused by faster removal of O_3 precursor species at lower flight levels, whereas atmospheric residence times of O_3 precursors are longer at higher altitudes, resulting in a more efficient accumulation. *Stordal et al.* [2006] found in their discussion paper a reduction of CH_4 lifetimes for lower flight altitudes, whereas in the case of higher flight altitudes methane lifetime changes were not consistent with respect to sign within the ensemble of four models, possibly because of the large differences in the model set-ups (*Stordal et al.* [2006] and corresponding interactive discussion). *Köhler et al.* [2008] found the largest CH_4 lifetime reduction for additional emissions in the upper troposphere, where ozone production is large and downward transport to lower altitudes and latitudes (with high ambient water vapor and photolysis rates) is efficient. *Grewe and Stenke* [2008] found maximum impact on CH_4 lifetime for emissions in the stratosphere and the tropical mid-troposphere. Minimum impact was found at tropopause levels, where OH formation is limited because of reduced water vapor concentration or UV radiation.

[6] It is clear from the above mentioned results, that there exists a considerable potential for mitigating non-CO_2 air traffic climate impact by adjusting flight paths to their minimum effect. Within this paper, a detailed assessment of the altitudinal dependency of major air traffic-induced perturbations and their climate effects is made. Effects on contrails and chemical perturbations (H_2O, O_3, CH_4) are calculated simultaneously within one model, so that all effects can be compared and traded-off against each other in a consistent way. The possible range of future effects with respect to temperature response is investigated, and particular focus is put on trade-offs between partially compensating effects from components acting on different timescales. We deliberately refrain from including direct aerosol effects, which are small according to the recent assessment from *Lee et al.* [2009]. Furthermore, we exclude contrail cirrus and indirect aerosol effects, which are potentially large. However, respective modeling tools have only recently been developed [*Liu et al.*, 2009; *Hendricks et al.*, 2009; *Burkhardt and Kärcher*, 2011; *Jacobson et al.*, 2011; *Schumann*, 2012] and results are still associated with high uncertainty particularly with respect to indirect aerosol effects. The current status of knowledge does not yet allow the inclusion of indirect aerosol effects in a flight altitude sensitivity study.

[7] For the present study, scenarios with standard and globally relocated cruise altitudes to higher or lower flight levels are applied. Changes in contrail coverage, chemical perturbations and radiative forcing are calculated by means of global three-dimensional atmospheric chemistry climate model simulations. Future development of radiative forcing and temperature response for all flight altitude change scenarios is calculated for different future scenarios by means of a simple climate response model. Trade-offs between partially compensating effects from various chemical species and contrails and from short-term and long-term effects are considered.

[8] Changing flight altitudes globally without any regional or seasonal adjustment is a theoretical and simplified approach. However, it helps to understand fundamental interdependencies between the most important contributors to radiative forcing and climate change and gives a thorough impression of the sensitivities and the potential, when trying to mitigate aviation climate impact through flight altitude changes. For a more sophisticated approach regional and seasonal effects or even actual meteorological conditions should be considered, as e.g. within the ongoing EU FP7 project REACT4C, http://www.react4c.eu).

2. Air Traffic Data and Future Scenarios

[9] Within the present study a global three-dimensional air traffic emission inventory with standard flight altitudes and alternative scenarios with globally relocated mean flight altitudes toward higher or lower levels are employed. These were established within the EU FP5 Project TRADEOFF and were used within other studies [e.g., *Fichter et al.*, 2005; *Gauss et al.*, 2006; *Fichter*, 2009; *Frömming et al.*, 2011]. The global fleet of aircraft is represented by 16 aircraft-engine combinations. Fuel flow profiles for these representative aircraft types were computed by means of the commercial aircraft performance model PIANO (http://www.piano.aero). The total amount and frequency of movements between city pairs was determined from flight track data from the EUROCONTROL and FAA air space and from scheduled flight data for the rest of the world [*Gardner et al.*, 1997]. The inventories are generated by assigning a global database of aircraft movements to corresponding fuel-flow profiles by means of the FAST model [*Kingdon*, 2000], assuming great circle routes between city pairs. This results in three-dimensional gridded data of fuel consumption, NO_x emissions and flown distances, provided as seasonal means with a horizontal resolution of $1^\circ \times 1^\circ$ and a vertical resolution of 2000 ft (~610 m), resembling the separation distance of real flight levels. A more detailed description of the data can be found in, e.g., *Gauss et al.* [2006] and *Fichter* [2009]. Table 1 gives the annual global mean values of distance flown, fuel consumption and NO_x emission for the year 2000. The TRADEOFF 2000 inventory is consistent with more recent air traffic inventories, e.g. the FAA inventory for the year 2006 [*Wilkerson et al.*, 2010], implying an annual growth rate of 3.6% per year between 2000 and 2006. The regional distribution of fuel consumption in TRADEOFF 2000 as shown in *Gauss et al.* [2006] compares well with the

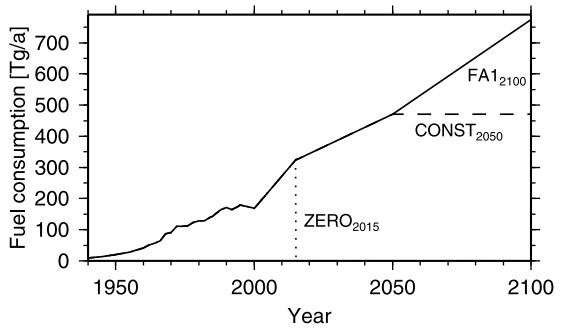

Figure 1. Temporal development of fuel consumption for three simplified air traffic future scenarios.

FAA inventory; only over long-distance flight corridors the difference between great circle routes in TRADEOFF 2000 and recorded flight position and dispersed great circle distances in *Wilkerson et al.* [2010] becomes obvious. The peak fuel consumption occurs between 9 and 11 km altitude in the TRADEOFF inventory, whereas the peak CO_2 emission lies between 10 and 12 km in the FAA inventory. The vertical distribution of traffic density in the TRADEOFF inventory was compared to the AERO2K inventory in *Frömming et al.* [2011], which shows a similar altitudinal distribution as the FAA inventory. The impact of vertically different air traffic density on contrail radiative forcing was found to be small (3%) [*Frömming et al.*, 2011]. The impact of vertically different air traffic density on O_3 radiative forcing has been studied by *Dahlmann* [2012] and was also found to be very small (2%).

[10] In addition to the inventory with standard flight altitudes (base case), four scenarios with globally relocated mean flight altitudes toward higher or lower flight levels were provided. Starting from the base case inventory, the mean cruise altitude of each flight profile is gradually shifted toward higher or lower altitudes by increments of 2000 ft. Scenarios with 2000 ft higher, 2000 ft lower, 4000 ft lower and 6000 ft lower cruise altitudes have been generated. Changes in aerodynamics for changed flight levels and therefore additional or reduced fuel consumption were taken into account. Flight altitude changes only occurred if the respective aircraft was able to perform the particular flight in terms of air frame restrictions and fuel capacity. In the lower flight altitude scenarios, ~1% of flights (in terms of distance traveled) could not be displaced from the main cruise level to the respective lower level. For the +2000 feet scenario, ~10% of flights had to be excluded from a replacement to the higher flight level. An overview of the scenarios is given in Table 1.

[11] The future climate impact of changes in flight altitude and the corresponding tradeoffs between short-term and long-term, positive and negative component effects depend crucially on the future development of emissions. To illustrate the possible range of future developments we chose three simplified theoretical future scenarios (business as usual, zero growth rates, zero air traffic). Future air traffic growth rates develop: (1) according to the Fa1 scenario (FESG IS92a1 [*Penner et al.*, 1999]) until 2050, extended to 2100 using medium growth rates between 2000 and 2050 (FA1$_{2100}$); (2) according to the Fa1 scenario until 2050 and constant emissions from 2050 onwards (CONST$_{2050}$); and (3) according to the Fa1 scenario until 2015 and zero emissions from 2015 onwards (ZERO$_{2015}$).

[12] The development of fuel consumption for these three scenarios is shown in Figure 1. We assume globally homogeneous growth rates. Alternative flight altitudes from the TRADEOFF flight level change scenarios are introduced in the year 2000 and are maintained from then onwards. The range of future scenarios is chosen broad enough so that future developments would most likely lie within this range, although it might be possible, that aviation grows faster than business as usual. The background CO_2 concentration is assumed similar to *Sausen and Schumann* [2000].

3. Model Description

[13] Aviation-induced changes in contrails, chemical species and related radiative forcings were calculated by means of the three-dimensional atmospheric chemistry climate model ECHAM4.L39(DLR)/CHEM/ATTILA (hereafter E39CA) [*Stenke et al.*, 2009], which is employed in a CTM-like mode in the present study. Based on the results of E39CA for the reference year 2000, the temporal development of global mean radiative forcing and surface temperature until 2100 is calculated by means of the simple climate response model AirClim [*Grewe and Stenke*, 2008]. Both models are briefly described in the following Sections.

3.1. The Atmospheric Chemistry Climate Model E39CA

[14] The atmospheric chemistry climate model E39CA [*Stenke et al.*, 2009] is an upgraded version of ECHAM4.L39(DLR)/CHEM (E39C) [*Hein et al.*, 2001], using the fully Lagrangian advection scheme ATTILA [*Reithmeier and Sausen*, 2002] for the transport of water vapor, cloud water and chemical trace species instead of the semi-Lagrangian advection scheme of *Williamson and Rasch* [1994]. E39CA is based on the general circulation model ECHAM4 [*Roeckner et al.*, 1996] being coupled to the chemistry module CHEM [*Steil et al.*, 1998]. The chemistry module makes use of the family concept and includes stratospheric homogeneous and heterogeneous ozone chemistry and the most relevant chemical processes describing the tropospheric background chemistry by means of 107 photochemical reactions, 37 chemical species and 4 heterogeneous reactions on polar stratospheric clouds (PSCs) and on sulfate aerosols. The radiation scheme used within E39CA is based on the radiation scheme from the ECMWF forecast model [*Fouquart and Bonnel*, 1980; *Morcrette*, 1991], including several updates as described in *Stuber et al.* [2001] and *Marquart and Mayer* [2002]. For the present study the model is run in CTM-like mode, in which concentration changes from chemical species do not feedback onto radiation and dynamics. Therefore the meteorological situation is identical in all simulations and statistically significant results can be obtained for a simulation period of only a few years after spin-up. For the present study 3-year means are analyzed, representing conditions of the year 2000. Statistical significance has been tested for the base case and is assumed to be similar for the flight altitude change scenarios. The model is

employed with a vertical resolution of 39 levels with the top level centered around 10 hPa and a spectral horizontal resolution of T30 (corresponding to a Gaussian grid of ~3.75° × 3.75°). A parameterization for line-shaped contrails [*Ponater et al.*, 2002] is included, which is based on the thermodynamic theory of contrail formation [*Schumann*, 1996]. Aviation water vapor perturbations are determined by tagging aviation water vapor emissions, which experience loss processes through cloud physics, rainout, and chemical conversion, proportional to natural water vapor. Ozone perturbations are determined by analyzing the difference between two simulations. The stratosphere-adjusted radiative forcing at the tropopause is calculated using the method developed by *Stuber et al.* [2001]. With respect to ozone, the performance of the radiation code is in close agreement with a narrow band model [*Stuber et al.*, 2001; *Forster et al.*, 2001]. A benchmark test with respect to contrail radiative forcing was accomplished in *Frömming et al.* [2011] and the net radiative forcing of 140 mWm^{-2} was found to be close to the multimodel mean of 144 mWm^{-2} as given by *Myhre et al.* [2011]. The water vapor radiative forcing was found to be underestimated in comparison with a narrow band model and was corrected accordingly [*Forster et al.*, 2001].

[15] Most validation studies have been performed with E39C [e.g., *Hein et al.*, 2001; *Grewe et al.*, 2001; *Brunner et al.*, 2003, 2005]. O_3, CO, and OH were found to be generally in good agreement with observations. Specific emphasis was put on the representation of NO_x mixing ratios in the North Atlantic flight corridor, since these values are crucial for the chemical impact of air traffic emissions. Model data were compared to in-situ measurements on-board a commercial aircraft [*Grewe et al.*, 2001]. The frequency distribution of occurring mixing ratios, i.e. the most frequent values and their seasonality was shown to be well represented. However, HNO_3 appears to be overestimated by up to a factor of about 2 in the tropical upper troposphere because of missing background NMHC (non-methane hydrocarbon) chemistry in E39C, as too much NO_x is converted to HNO_3 instead of other reservoirs such as PAN. However, results lie within the range of other models [*Brunner et al.*, 2003, 2005]. *Kentarchos and Roelofs* [2002] have studied the impact of NMHC chemistry on aviation-induced ozone and found ~10% higher ozone perturbation when NMHC chemistry was included.

[16] The purely Lagrangian transport scheme ATTILA is numerically non-diffusive, resulting in a significant reduction of systematic model biases in the upper troposphere and lower stratosphere region from E39C to E39CA [*Stenke et al.*, 2008, 2009]. Simulated water vapor mixing ratios in the lowermost stratosphere were overestimated in E39C by a factor 3–5 compared with observations, but are reduced in E39CA by up to 70% [*Stenke et al.*, 2008], and agree much better with observations. The temperature bias in the extra tropical lowermost stratosphere of more than 7 K in E39C is substantially reduced by more than 50% in E39CA [*Stenke et al.*, 2008], also yielding a better representation of the simulated tropopause height [*Stenke et al.*, 2008]. *Frömming et al.* [2011] exemplarily show that in comparison with ERA40 data, relative humidity over ice is reproduced much better in E39CA than in E39C. The distribution of chemical trace species is generally better in accordance with measurements [*Stenke et al.*, 2009].

[17] The model has been applied in numerous studies investigating chemical perturbations from aircraft emissions and contrails [e.g., *Grewe et al.*, 2002a; *Marquart et al.*, 2003; *Frömming et al.*, 2011], and was found to agree well with other studies, as will be shown in detail in Section 4.

3.2. The Linear Climate Response Model AirClim

[18] AirClim is a simple climate response model [*Grewe and Stenke*, 2008], which is employed for the assessment of the global climate impact of air traffic emissions. It is based on the linear climate response model of *Hasselmann et al.* [1993], which was modified by *Sausen and Schumann* [2000] and has been updated and further extended by *Grewe and Stenke* [2008] to cover additional species. In the present work, the aviation-induced perturbations and the associated radiative forcings are determined beforehand by E39CA simulations, and AirClim is used subsequently to calculate the temporal development of global mean radiative forcing and temperature change according to selected future scenarios, for which we assume globally homogeneous growth rates. This is of course a simplifying assumption. However, an inclusion of regionally different growth rates would require a regional resolution of the linear response model. In addition it would obscure the effects of flight altitude changes and complicate the analysis of tradeoffs between short-term and long-term effects. The future radiative forcing of the short-lived species is assumed to scale linearly according to the temporal development of the emissions. This implies, that potential changes in background climate would not affect e.g. the distribution of contrails or ozone perturbation and the respective radiative forcings. This is a reasonable assumption, as shown by *Marquart et al.* [2003] for contrail coverage and by *Grewe et al.* [1999] for aviation ozone. The global mean CO_2 concentration change from air traffic CO_2 emissions is determined by means of an impulse response function according to *Hasselmann et al.* [1997] and *Sausen and Schumann* [2000], taking the long lifetime and accumulation effects of historic and future emissions into account. The radiative forcing (RF) from air traffic induced CO_2 is calculated according to *Intergovernmental Panel on Climate Change* [2001]. The aviation-induced CH_4 lifetime change resulting from NO_x emissions is derived from the change in tropospheric OH concentrations as simulated by E39CA. The perturbation of the CH_4 concentration through air traffic is assessed following *Grewe and Stenke* [2008], which then allows the calculation of the aviation-induced methane radiative forcing according to *Intergovernmental Panel on Climate Change* [2001]. Being an important ozone precursor, the air traffic induced methane reduction entails a small but long-term reduction in ozone (O_{3L}, hereafter), which sometimes also is referred to as the primary mode ozone change (PMO). For our model system we determine this effect to be a factor of 0.29 of the methane radiative forcing. This factor was derived by comparing changes in the ozone mixing ratios in simulations with and without aviation emissions, as explained in detail by *Dahlmann* [2012]. The factor for the inclusion of primary mode ozone by scaling methane radiative forcing lies within the range of other studies [e.g., *Stevenson et al.*, 2004; *Hoor et al.*, 2009; *Wild et al.*, 2001; *Köhler et al.*, 2008], which determined the factor to be 0.23, 0.42, 0.47, and 0.58, respectively.

Table 2. Climate Sensitivity Parameter λ (K/(Wm^{-2})) and Efficacy Parameter r_{eff} for Aviation Emissions as Determined From ECHAM4/MLO Equilibrium Climate Change Simulations[a]

Species	CO_2	O_3	CH_4	H_2O	Contrails
λ	0.73	1.00	0.86	0.83	0.43
r_{eff}	1.00	1.37	1.18	1.14	0.59

[a]*Ponater et al.* [2006].

[19] The transient changes of the global mean surface temperature response (ΔT) from the radiative forcing changes determined above are calculated by means of the Green's function (G_T) of the surface temperature response according to *Sausen and Schumann* [2000]. As the function was fitted to reproduce the performance of a global atmosphere-ocean circulation model, the response time (τ) comprises the response times of the surface layer and the deep ocean, with α = 2.246 K/36.8 yr, and τ = 36.8 yr:

$$\Delta T(t) = \int_{t0}^{t} G_T(t-t') \cdot RF^*(t')dt' \quad (1)$$

$$G_T(t-t') = \alpha \cdot e^{(t-t')/\tau} \quad (2)$$

$$RF^*(t) = \frac{RF_i(t)}{RF_{CO2}} \cdot \frac{\lambda_i}{\lambda_{CO2}} \quad (3)$$

RF* is the radiative forcing of species (i) normalized to the radiative forcing of CO_2, considering the distinctive climate sensitivity (λ_i) of each species, i.e. its efficacy [*Hansen et al.*, 2005]. The surface temperature response thus includes the individual efficacy parameters $r_{eff} = \lambda_i/\lambda_{CO2}$ for air traffic perturbations as determined by *Ponater et al.* [2006] and given in Table 2. It has not been studied yet, whether efficacies might change in response to a flight altitude change. We assume the same efficacies for changes in flight altitudes, as has been done by *Schwartz Dallara et al.* [2011].

[20] The advantage of using AirClim for assessing transient temperature development is, that it reproduces the deterministic component of the underlying comprehensive climate model. No internal variability is simulated, rendering statistical tests for temperature changes unnecessary. As relatively small component forcings and responses are considered within the present study, this methodology is deliberately chosen to avoid detection problems or the necessity of scaling, which is unavoidable when using full-range climate models in order to obtain statistically significant climate responses for small perturbations [e.g., *Olivié et al.*, 2012]. However, physical uncertainties of the relevant input parameters are taken into account in terms of uncertainty ranges for radiative forcings and efficacies for all species and methane perturbation lifetime, as has been done by *Grewe and Stenke* [2008]. An uncertainty range of ±5% is assumed for CO_2 radiative forcing, ±10% for CH_4 radiative forcing, ±30% for O_3 radiative forcing, ±50% for H_2O and contrail radiative forcing, ±40% uncertainty is assumed for CH_4 perturbation lifetime. For efficacies an uncertainty range of ±30% is included for H_2O and O_3 and ±10% for CH_4 and contrails. Anomalous efficacies ($r_{eff} \neq 1$) are not well established at this stage, thus the given uncertainty ranges include efficacies of 1 for all species except contrails, as for the latter all available studies unanimously indicate substantially reduced r_{eff} of contrails compared to CO_2 [*Ponater et al.*, 2006; *Rap et al.*, 2010a]. All parameter combinations were accounted for by means of a Monte Carlo simulation, thus a range of uncertainty for radiative forcing and temperature change can be given.

4. Aviation Impact of the TRADEOFF Base Case

[21] The global coverage with line shaped contrails for the TRADEOFF 2000 base case is 0.19% for all contrails and 0.09% for visible contrails, yielding a radiative forcing of 5.9 mW/m^2. More detailed results can be found in *Frömming et al.* [2011]. The radiative forcing of linear contrails lies within the range of other recent studies, ranging from 2.8 mW/m^2 [*Stuber and Forster*, 2007] to 12 mW/m^2 [*Rap et al.*, 2010b] for air traffic in 2002 and from 5.4 mW/m^2 to 25.6 mW/m^2 for air traffic in 2005 [*Lee et al.*, 2009].

[22] The perturbation of water vapor mixing ratios by present-day subsonic air traffic water vapor emissions has found to be less than 1% of background water vapor. Figure 2 shows the zonal annual mean perturbation with an annual average maximum perturbation of 39 ppb at about 60°N, just above the tropopause. The net radiative forcing of water vapor is 1.5 mW/m^2. The results are in good agreement with earlier studies investigating future subsonic air traffic water vapor effects [e.g., *Penner et al.*, 1999; *Marquart et al.*, 2001; *Gauss et al.*, 2003], taking into account that different emission inventories were employed.

[23] The NO_x emissions from global air traffic in 2000 cause a maximum perturbation of about 80 pptv in the annual zonal mean. The enhanced NO_x levels entail an increase of total global ozone column by 0.48 DU and a maximum increase of O_3 mixing ratios of 4.5 ppbv in the annual mean (Figure 3). The present results are in good agreement with other recent studies, which report an increase of O_3 column between 0.39 and 0.65 DU [*Myhre et al.*, 2011], and annual mean peak O_3 mixing ratios between 3.7 ppbv [*Hoor et al.*, 2009] and 6–9 ppbv [*Köhler et al.*, 2008] for similar air traffic inventories. The O_3 radiative forcing for the TRADEOFF 2000 inventory is 14.7 mW/m^2, resulting in a specific radiative forcing of

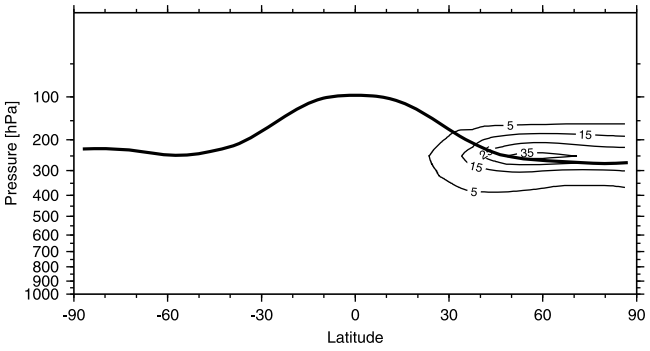

Figure 2. Zonal annual mean air traffic induced water vapor (ppb) for the TRADEOFF base case. The bold line indicates the simulated annual mean tropopause height.

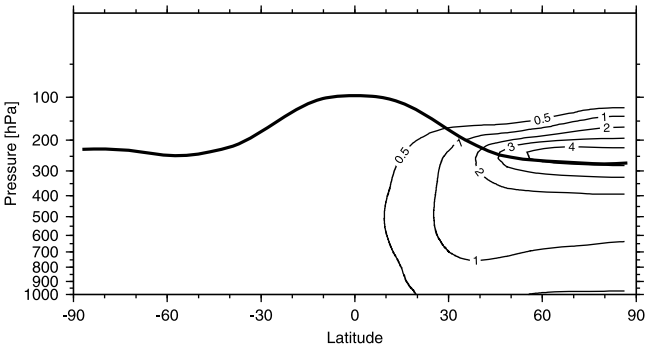

Figure 3. Zonal annual mean air traffic induced ozone (ppbv) for the TRADEOFF base case. The bold line indicates the simulated annual mean tropopause height.

24.5 $mWm^{-2}/Tg(N)yr^{-1}$. This agrees well with other studies reporting O_3 radiative forcing from 12–28 mW/m^2 [*Sausen et al.*, 2005] and 13–21 mW/m^2 [*Myhre et al.*, 2011] for slightly different emission inventories, and specific radiative forcings of 36.9 $mWm^{-2}/Tg(N)yr^{-1}$ [*Lee et al.*, 2010] and 27.3 ± 9.7 $mWm^{-2}/Tg(N)yr^{-1}$ [*Holmes et al.*, 2011] as well as ranges from 16–25 $mWm^{-2}/Tg(N)yr^{-1}$[*Myhre et al.*, 2011]. *Köhler et al.* [2008] found somewhat larger O_3 radiative forcing of 30 mW/m^2, corresponding to 45 $mWm^{-2}/Tg(N)yr^{-1}$, whereas *Unger* [2011] report much smaller aviation-induced O_3 radiative forcing of only 6 mW/m^2, corresponding to 8 $mWm^{-2}/Tg(N)yr^{-1}$.

[24] NO_x emissions and O_3 enhancement yield an increase of the OH concentration. As the main loss process for tropospheric CH_4 is the reaction with OH, this in turn results in a reduction of CH_4 lifetime. We derive a CH_4 lifetime reduction of 0.714% (including a feedback factor of 1.4 for an equilibrium response [e.g., *Fuglestvedt et al.*, 1999]), which is slightly smaller than reported from other recent studies. *Hoor et al.* [2009] calculated aviation-induced CH_4 lifetime reduction ranging from 0.69% to 1.8% with a mean value of 1.04% (without feedback). *Myhre et al.* [2011] give a range of CH_4 lifetime reduction between 0.81% and 1.57% (without feedback), whereas *Köhler et al.* [2008] calculated much larger CH_4 lifetime changes of 3% (including feedback). *Lee et al.* [2010] report normalized CH_4 lifetime reduction of 1.9 ± 0.9%/$Tg(N)yr^{-1}$.

5. Atmospheric Impact of Global Changes of Flight Altitudes

5.1. Effects on Contrails

[25] The effect of flight altitude changes on contrails and contrail radiative forcing has been discussed in detail by *Fichter et al.* [2005]. In that study the previous model version E39SLT and the TRADEOFF scenarios for the year 1992 were used, whereas in the present study, the updated model version E39CA and the TRADEOFF scenarios for the year 2000 have been applied. The qualitative effects of global mean flight altitude changes on contrails and their radiative forcing remain similar, but are reconsidered here to emphasize the complexity of the contrail response to flight altitude shifting in comparison with other effects.

[26] Figure 4 shows the zonal mean contrail coverage for all flight altitude scenarios (Figure 4, left) and the changes in contrail coverage with respect to the base case (right). The change pattern shows a distinct zonal variation, which is mainly caused by the distribution of contrail supporting regions [see *Frömming et al.*, 2011]. At tropical and subtropical latitudes, flying lower reduces contrail coverage because of higher ambient temperatures preventing condensation during the mixing of exhaust and ambient air, whereas more contrails can form when flying at higher altitudes in the tropics and subtropics, as air traffic is shifted into the upper troposphere where supersaturation is more frequent. At polar latitudes, flying higher yields a decrease of contrail coverage, as a larger fraction of air traffic is relocated into the stratosphere where supersaturation is rare. In contrast, flying lower slightly increases contrail coverage at polar latitudes, because a part of the high altitude air traffic is shifted from the dry stratosphere into the troposphere. In the mid latitudes, the effect of relocating flight altitudes depends strongly on seasonal and synoptic conditions (Figure S1, auxiliary material).[1] Results for global

[1]Auxiliary materials are available in the HTML. doi:10.1029/2012JD018204.

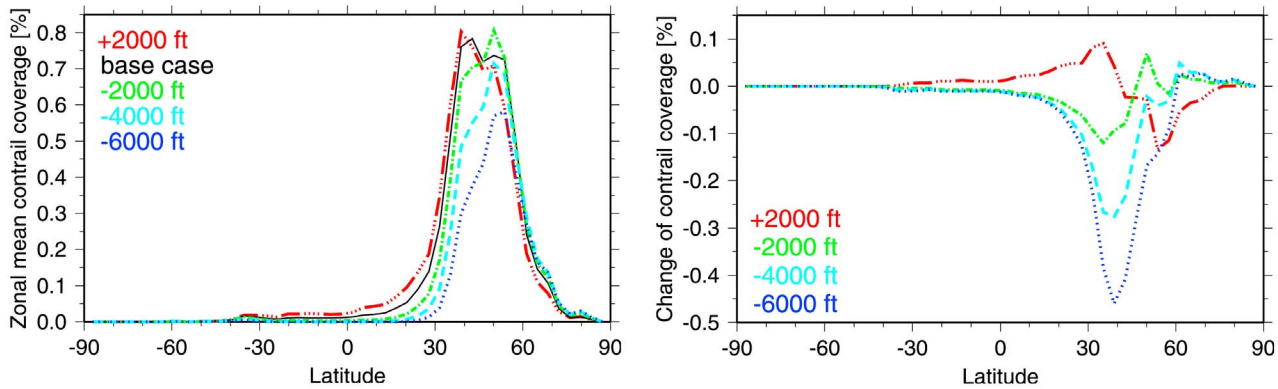

Figure 4. (left) Zonal annual mean contrail coverage for all TRADEOFF scenarios and (right) absolute changes of the zonal annual mean contrail coverage through a displacement of flight altitudes by 2000 ft up and 6000 ft down.

Table 3. Global Annual Mean Visible Contrail Coverage, Aviation-Induced Water Vapor, Contribution to the Total Ozone Column and CH_4 Lifetime Changes (Including Feedback Factor) for the Base Case and the Flight Altitudes Change Scenarios

Scenario	Visible Contrail Coverage (%)	Aviation H_2O (Tg)	Contribution to the Total O_3 Column (DU)	CH_4 Lifetime Change (%)
+2000 ft	0.102	11.4	0.53	−0.712
Base case	0.090	10.0	0.48	−0.714
−2000 ft	0.085	8.8	0.44	−0.719
−4000 ft	0.068	8.1	0.41	−0.811
−6000 ft	0.045	7.6	0.38	−0.835

annual mean contrail coverage are given in Table 3. On global annual average, the contrail coverage decreases for lower flight altitudes and increases for higher flight altitudes.

[27] Only line-shaped contrails are included in this study. As the spatial distribution of contrail cirrus differs from that of line-shaped contrails [*Burkhardt and Kärcher*, 2011], there is no guarantee that the changes of line shaped contrails in response to flight altitude changes will translate to contrail cirrus, or that the enhancement factor of contrail cirrus with respect to young contrails would be transferable to the flight altitude mitigation scenarios. Hence, any scaling of changes in line-shaped contrails resulting from changes in flight altitudes to contrail cirrus appears to be inadequate.

5.2. Effects on H_2O

[28] Figure 5 shows zonal annual mean changes of air traffic induced water vapor mixing ratios resulting from globally displaced flight altitudes, for the 2000 ft higher and the 6000 ft lower flight altitudes. Higher flight altitudes yield an increase of water vapor mixing ratios, whereas lower flight altitudes yield a decrease of water vapor mixing ratios. This is consistent with the findings of *Gauss et al.* [2003] for different altitudes of water vapor emissions from cryoplanes. When flying higher, a larger fraction of water vapor is emitted in the stratosphere, where the emissions can accumulate to larger concentration changes. In the zonal mean, the peak perturbation of aviation-induced water vapor increases from 39 ppb to 45 ppb in the +2000 ft case compared with the base case. In the scenarios with lower flight altitudes, the peak perturbation gradually decreases to 27 ppb, 15 ppb, and 12 ppb for −2000 ft, −4000 ft, and −6000 ft, respectively. The total amount of accumulated water vapor is given in Table 3 for all flight altitudes.

5.3. Effects of NO_x on O_3 and CH_4

[29] The effect of flight altitude changes on the aviation-induced NO_x and O_3 perturbation has been studied earlier by *Grewe et al.* [2002b] for a 1 km lower flight altitude and by *Gauss et al.* [2006] for flight altitude changes by +2000 ft and −6000 ft. The change patterns as well as the magnitudes of chemical changes found within the present study (Figures 6, 7, and 8) agree very well with these earlier studies. The availability of the −2000 ft and −4000 ft offers additional possibilities to understand the cause and effect relationships and allows investigating the degree of linearity of the response to flight altitude changes.

[30] Figure 6 shows the effect of flight altitude changes on NO_x mixing ratios with respect to the base case. When flying higher, NO_x mixing ratios increase at 200 hPa by nearly 30 pptv, which is accompanied by a small decrease of NO_x at around 300 hPa. For 6000 ft lower flight altitudes, a strong decrease of NO_x mixing ratios is found at about 250 hPa, whereas below NO_x mixing ratios increase by a much smaller extent, even though in total more NO_x is emitted in the lower flight altitude scenario (Table 1). This can be associated with the decrease of NO_x lifetimes with

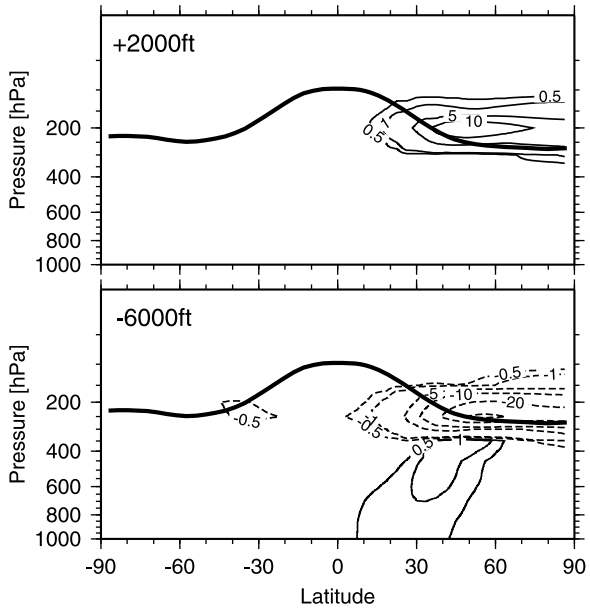

Figure 5. Changes of the zonal annual mean aviation-induced water vapor mixing ratios (ppb) through a displacement of flight altitudes by 2000 ft up and 6000 ft down. The bold line indicates the annual mean tropopause height.

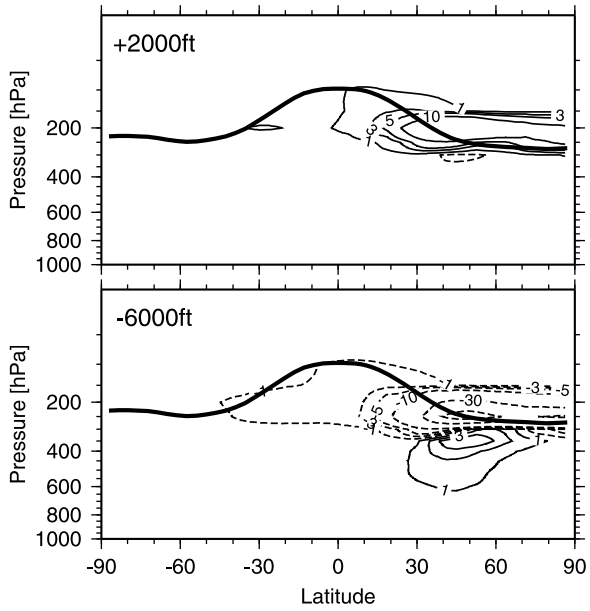

Figure 6. Changes of the zonal annual mean aviation-induced NO_x mixing ratios (pptv) through a displacement of flight altitudes by 2000 ft up and 6000 ft down. The bold line indicates the annual mean tropopause height.

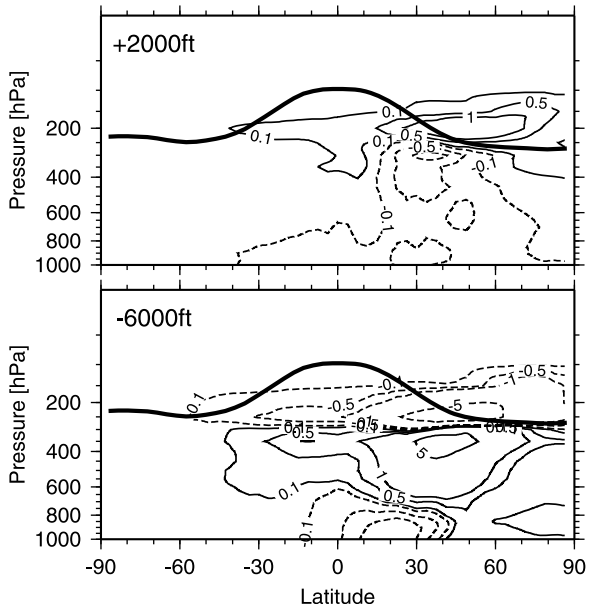

Figure 7. Changes of the zonal annual mean aviation-induced net O_3 production (10^3 molecules $cm^{-3}s^{-1}$) through a displacement of flight altitudes by 2000 ft up and 6000 ft down. The bold line indicates the annual mean tropopause height.

decreasing altitude. If NO_x is emitted at lower tropospheric levels, the emissions have a shorter residence time, hence mixing ratios increase by a smaller extent compared with the decrease above. At higher altitudes, NO_x emissions can accumulate and mixing ratios increase in a disproportionate way compared with the decrease below.

[31] The pattern of net ozone production changes (Figure 7) is more complex, as it is a composite of several individual processes. Corresponding figures on O_3 loss, O_3 production and HO_2 change can be found in the auxiliary material (Figures S2 and S3). In case of lower flight altitudes, the decrease of NO_x at higher altitudes results in reduced conversion of HO_2 to OH. The O_3 production decreases because of lower NO_x, and the O_3 loss increases because of enhanced HO_2, which yields a net reduction of O_3 production at standard flight levels. The opposite is true for the increase of NO_x at lower levels, which results in more efficient conversion of HO_2 to OH and accordingly higher net O_3 production. Because of increasing O_3 lifetime with height, the enhanced net O_3 production at lower altitudes is overcompensated through the reduced net O_3 production at higher altitudes. This yields a decrease of O_3 mixing ratios in the upper troposphere for lower flight altitudes (Figure 8).

[32] For higher flight altitudes, NO_x mixing ratios increase at higher levels and slightly decrease at lower levels. These changes are accompanied by the inverse changes of HO_2 through a more or less efficient conversion of HO_2 to OH. The increase of NO_x at higher altitudes entails an increase of O_3 production, whereas the decrease of HO_2 yields a reduction of O_3 loss, together leading to an increase of net O_3 production at higher altitudes as evident in Figure 7. At lower altitudes the decrease of NO_x yields an increase of HO_2, which in turn reduces the O_3 production. Together with transport and mixing, the changes at higher altitudes dominate the total effect, leading to an overall increase of O_3 mixing ratios for higher flight altitudes as shown in Figure 8. The aviation-induced contribution to the total O_3 column decreases gradually for lower flight altitudes, whereas it increases for higher flight altitudes (Table 3).

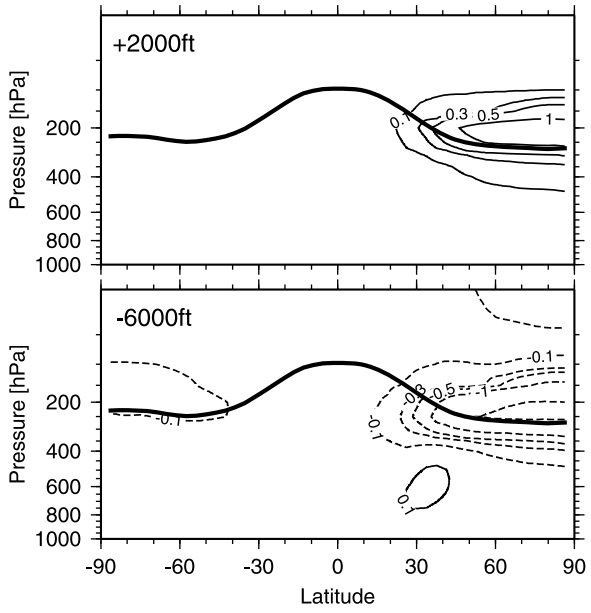

Figure 8. Changes of the zonal annual mean aviation-induced O_3 mixing ratios (ppbv) through a displacement of flight altitudes by 2000 ft up and 6000 ft down. The bold line indicates the annual mean tropopause height.

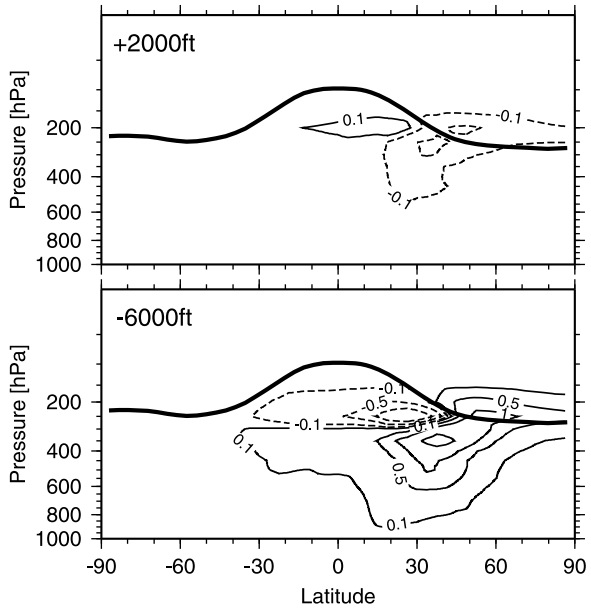

Figure 9. Changes of the zonal annual mean aviation-induced OH concentration (10^4 molecules cm^{-3}) through a displacement of flight altitudes by 2000 ft up and 6000 ft down relative to the base case. The bold line indicates the annual mean tropopause height.

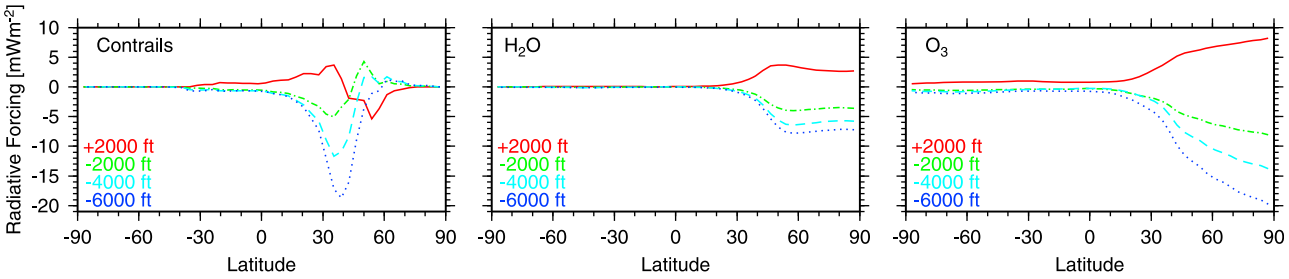

Figure 10. Changes of the zonal annual mean net radiative forcing (mW/m^2) of contrails, H_2O, and O_{3S} through flight altitude changes by 2000 ft up, 2000 ft down, 4000 ft down, and 6000 ft down.

[33] Figure 9 shows OH concentration changes for the +2000 ft and the −6000 ft case. For lower flight altitudes, the decrease of NO_x mixing ratios at standard flight levels (Figure 6) results in reduced HO_2 to OH conversion, reducing OH at low latitudes, whereas in the lowermost stratosphere at mid to polar latitudes both HO_2 and OH increase. In the tropical lower troposphere, OH increases because of higher levels of O_3, which allow more O_3 to be photolyzed, producing additional OH. In the remaining troposphere, higher NO_x emissions yield a more efficient HO_2 to OH conversion and therefore an increase of OH. In total, the global mean OH concentration increases for lower flight altitudes, which results in a reduction of methane lifetime compared with the base case (Table 3). For higher flight altitudes, the inverse pattern of OH changes is found: NO_x emissions increase at higher altitudes yielding an increase in OH at low latitudes, whereas at mid and polar latitudes, OH concentration decreases. In the troposphere at lower latitudes, the decrease of NO_x mixing ratios entails a reduction of OH. In total, higher flight altitudes yield a reduction of OH concentration, which results in a small increase of methane lifetimes compared with the base case. Methane lifetime changes are summarized for all scenarios in Table 3.

5.4. Effects on CO_2

[34] Changes in fuel consumption through flight altitude changes as given in Table 1 propagate linearly onto CO_2 emissions. Because of the long atmospheric lifetime of CO_2, the effect of increased or reduced fuel burn transfers slowly into rising or falling global CO_2 concentration. It will become clear in Section 7, how the accumulative effect of CO_2 and the fast responding non-CO_2 effects compete with each other for various future scenarios.

6. Effects on Radiative Forcing

[35] Figure 10 shows the zonal mean radiative forcing of equilibrium changes of contrail, water vapor and ozone for the year 2000 for all flight altitude change scenarios. Consistent with the individual inhomogeneous change patterns of these short-lived effects, the radiative forcing changes are largely restricted to the northern hemisphere. Water vapor and ozone radiative forcings generally increase for higher flight altitudes and decrease for lower flight altitudes, whereas the zonal mean contrail radiative forcing changes show the same latitudinal structure as the changes of contrail coverage (Figure 4). In all cases, the tropical and subtropical changes outweigh the changes at mid latitudes because of the comparatively larger areas affected, resulting in global mean radiative forcing as given in Table 4. In relative terms, the global mean contrail radiative forcing increases by +6% for 2000 ft higher flight altitudes, but decreases by −13%, −30%, and −49% for 2000 ft, 4000 ft, and 6000 ft lower flight altitudes, respectively.

[36] Global mean radiative forcing changes of air traffic induced water vapor are comparatively small, as mainly latitudes north of 40°N are affected. Although, in absolute terms, water vapor causes the smallest radiative forcing compared to other subsonic aviation effects, the radiative forcing changes caused by flight altitude shifts are of comparable magnitude to the changes due to contrails and ozone (Table 4).

[37] The global annual mean net ozone radiative forcing increases for higher flight altitudes, and decreases for lower flight altitudes. In relative terms, the global mean net radiative forcing changes by +8% for 2000 ft higher flight altitudes, −6% for 2000 ft lower flight altitudes, −9% for 4000 ft lower flight altitudes, and −14% for 6000 ft lower flight altitudes compared to the base case (Table 4).

[38] In absolute terms, the ozone radiative forcing always remains the largest of the three component effects. The largest individual reduction, by 2.9 mW/m^2, arises from contrail changes in the −6000 ft lower flight altitude scenario. The largest increase, however, by +1.2 mW/m^2 results from ozone radiative forcing changes in the +2000 ft case.

[39] The changes in OH yield a reduction of methane lifetime for lower flight altitudes and a slight increase of methane lifetime for higher flight altitudes (Table 3). This results in a larger negative methane radiative forcing for lower flight altitudes, and a slightly smaller negative methane radiative forcing for higher flight altitudes compared with the base case. It is worth noting, that with respect to

Table 4. Global Annual Mean Net Radiative Forcing (mW/m^2) of Contrails, Water Vapor and Ozone for All TRADEOFF Scenarios With Flight Altitude Changes for the Year 2000[a]

Scenario	RF_{cont} (mW/m^2)	RF_{H2O} (mW/m^2)	RF_{O3} (mW/m^2)
+2000 ft	6.3 (+0.4)	2.1 (+0.6)	15.9 (+1.2)
Base case	5.9	1.5	14.7
−2000 ft	5.1 (−0.8)	0.9 (−0.6)	13.8 (−0.9)
−4000 ft.	4.1 (−1.8)	0.6 (−0.9)	13.4 (−1.3)
−6000 ft	3.0 (−2.9)	0.3 (−1.2)	12.7 (−2.0)

[a]Absolute radiative forcing changes relative to the base case are given in parentheses.

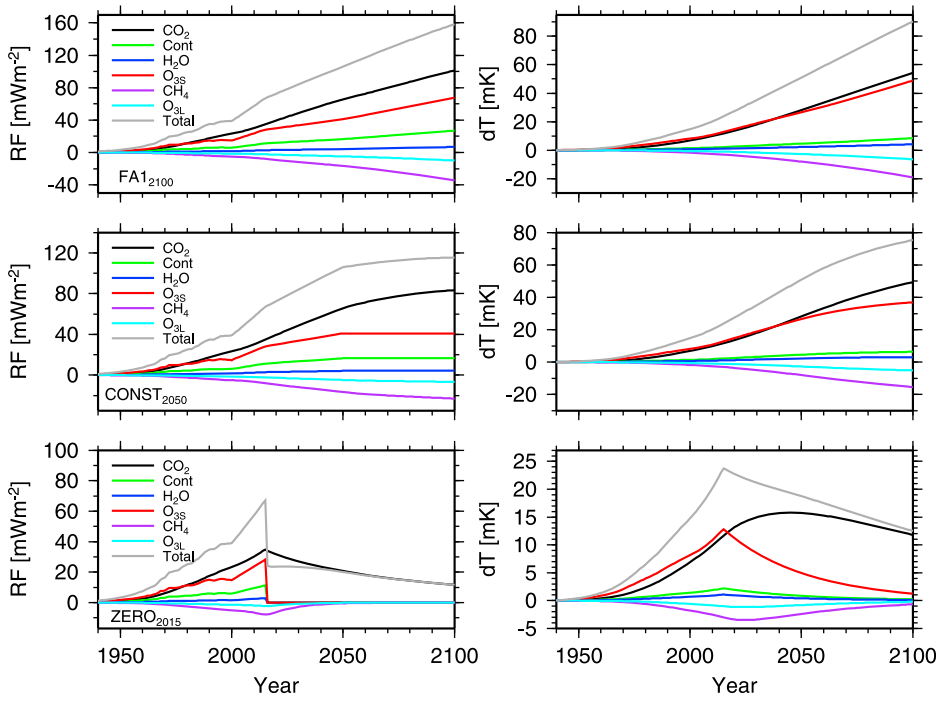

Figure 11. Temporal evolution of (left) radiative forcing (mW/m^2) and (right) surface temperature changes (mK) arising from contrails, H_2O, O_{3S}, CH_4, O_{3L} and CO_2 for the base case for the (top) $FA1_{2100}$, (middle) $CONST_{2050}$, and (bottom) $ZERO_{2015}$ future scenarios. Note the different scales for the axes of ordinates. Prior to 2000 the scenarios are identical. Figures for the flight altitude change scenarios are shown in the auxiliary material.

aviation in general, ozone imposes a positive radiative forcing and methane a negative radiative forcing, thus from a global mean perspective both effects partially compensate under equilibrium conditions. However, when flight altitudes are relocated, the net effect of both ozone and methane radiative forcing decreases for lower flight altitudes and increases for higher flight altitudes, thus, both work in the same direction.

[40] The CO_2 radiative forcing is larger for lower flight altitudes, as current aircraft are not optimized for these flight levels and hence consume more fuel. The effects of radiative forcing changes of the long-lived greenhouse gases CO_2 and CH_4 become significant only if accumulated over time, i.e. if the respective emission changes last for several years. The complex interrelationship between short and long-lived, positive and negative effects will become obvious in the following Section, and will be illustrated by means of three simplified theoretical future emissions scenarios.

7. Radiative Forcing and Surface Temperature Changes for Selected Future Scenarios

[41] The long-term effect of flight altitude changes on future radiative forcing and temperature response is demonstrated by means of three simplified theoretical future scenarios: one scenario with increasing emissions ($FA1_{2100}$), one scenario with constant emissions from 2050 onwards ($CONST_{2050}$) and one scenario with no emission after 2015 ($ZERO_{2015}$) (see Section 3.2 for details). For a consistent development of historic and future fuel consumption we have scaled all emissions of the year 2000 to the appropriate IEA aviation fuel statistics [*International Energy Agency*, 2007, Table 9]. Higher or lower flight altitudes are used alternatively to the base case from the year 2000 onwards. Transient radiative forcing and temperature response have been calculated by means of AirClim [*Grewe and Stenke*, 2008] (Section 3.2). The development of radiative forcing and temperature response for each future scenario is shown in Figure 11 for the base case. Additional figures for all flight altitude change scenarios and all future scenarios can be found in the auxiliary material (Figures S5, S6, and S7).

[42] For the $FA1_{2100}$ scenario, the magnitude of the radiative forcing of all species increases gradually until 2100 for all flight altitude cases (Figure 11 and auxiliary material Figure S5). The radiative forcing values are given in Table 5 for the year 2100. The total radiative forcing for the base case amounts to 158 mW/m^2, and increases for higher flight altitudes and reduces for lower flight altitudes. The reduction of radiative forcing for lower flight altitudes is dominated by contrails and methane, whereas the increase for higher flight altitude originates primarily from ozone radiative forcing. The CO_2 radiative forcing compensates the effects from the other species only to a very limited extent within the $FA1_{2100}$ future scenario. The respective temperature response in 2100 is given in Table 6. Figure 12 illustrates the respective contributions from each species to the radiative forcing and temperature changes in the year 2100. The change in temperature response from ozone increases in a disproportionate way compared with its radiative forcing change because of the larger efficacy parameter. For higher flight altitudes in the $FA1_{2100}$ scenario, the ozone induced

Table 5. Global Annual Mean Net Radiative Forcing (mW/m^2) for All TRADEOFF Scenarios in 2100 for an Increase of Air Traffic According to the $FA1_{2100}$ Scenario[a]

Scenario	Contrails	H_2O	O_{3S}	CH_4	O_{3L}	CO_2	Total
+2000 ft	29.1 (+2.1)	10.0 (+3.1)	73.6 (+6.2)	−34.1 (+0.3)	−9.8 (+0.1)	100.6 (−0.7)	169.3 (+11.1)
Base case	27.0	6.9	67.4	−34.4	−9.9	101.3	158.2
−2000 ft	23.5 (−3.5)	4.2 (−2.7)	63.4 (−4.0)	−40.7 (−6.3)	−11.7 (−1.8)	103.6 (+2.3)	142.4 (−15.8)
−4000 ft	19.0 (−8.0)	2.8 (−4.1)	61.5 (−5.9)	−46.8 (−12.4)	−13.5 (−3.6)	106.1 (+4.8)	129.2 (−29.0)
−6000 ft	14.0 (−13.0)	1.5 (−5.4)	58.4 (−9.0)	−49.8 (−15.4)	−14.4 (−4.5)	106.7 (+5.4)	116.4 (−41.8)

[a]Absolute radiative forcing changes relatively to the base case are given in parentheses.

temperature response is almost as large as that of CO_2 (Table 6 and auxiliary material Figure S5).

[43] The $ZERO_{2015}$ scenario instructively demonstrates the effect of emission reduction strategies, though it is unrealistic in this extreme form. It shows the characteristic tradeoffs between short-term and long-term effects and can be seen as an absolute minimum case of future development. The temporal development of the radiative forcing and temperature change for the base case is shown in Figure 11. For completeness, the development for all flight altitude change scenarios is shown in Figure S7 (auxiliary material). The changes with respect to the base case (Figure 13) reveal a combination of individual contributions caused by the different lifetimes of the effects: After the termination of emissions in 2015, the radiative forcing contributions of the short-lived species ozone, water vapor and contrails immediately drop to zero as soon as the perturbations disappear, whereas the associated temperature response starts to decrease slowly because of the inertia of the climate system. The CH_4 and O_{3L} radiative forcings decay exponentially with a perturbation lifetime of 12 years, the associated temperature response follows more slowly. After the disappearance of the methane radiative forcing, only the CO_2 radiative forcing remains, which is opposite in sign to the other effects, resulting in a reversal of the total radiative forcing change through altered flight altitudes between 2030 and 2040. Hence, beyond this reversal point, the radiative forcing change becomes slightly negative for higher flight altitudes and slightly positive for lower flight altitudes. The temperature response is characterized by the much longer response time of the climate system, such that the large response forced by the short-lived species declines only slowly, and the reversal point in temperature response from a negative to a positive temperature change and vice versa is reached beyond 2100.

[44] Figure 14 summarizes the total global net radiative forcing and temperature changes in 2100 due to higher or lower flight altitudes for all future scenarios. If business as usual was considered as high scenario and $ZERO_{2015}$ as low scenario, this would illustrate the range where future values would most likely lie in between. Uncertainties for radiative forcing, climate sensitivity and methane perturbation lifetime are included as described in Section 3.2 and the 95% confidence intervals are shown. We concentrate on differences to the base case. The differences are calculated for the same parameter combination for each flight altitude change scenario. Hence, the resulting uncertainty range corresponds to these differences and is rather narrow compared to the much larger uncertainty of the base case itself. For future scenarios with constant ($CONST_{2050}$) or increasing air traffic emissions ($FA1_{2100}$), the radiative forcing and temperature response changes through altered flight altitudes are dominated by the large contributions of the short-lived species ozone, water vapor, contrails and methane, i.e. the total net radiative forcing decreases for lower flight altitudes and increases for higher flight altitudes. If air traffic emissions are reduced or even terminated ($ZERO_{2015}$), the effects from the short-lived species decline and beyond a certain time horizon only the CO_2 effect remains, i.e. the total net radiative forcing increases slightly for higher flight altitudes and decreases for lower flight altitudes. Nevertheless, with respect to temperature change, the fading contribution from the short-lived species still controls the total effect in 2100 (Figures 13 and 14).

8. Conclusions

[45] The results from this study with respect to global changes of mean flight altitudes confirm earlier similar studies, which investigated flight altitude changes and their effects on contrails [e.g., *Fichter et al.*, 2005] or chemical perturbations [e.g., *Grewe et al.*, 2002b; *Gauss et al.*, 2006]. The present study addresses for the first time the tradeoffs caused by the simultaneous action of various impact components (contrails, H_2O, O_{3S}, CH_4, O_{3L}, CO_2) working on different timescales. It represents a detailed assessment of the major air traffic effects, trading off their partially counteracting effects against each other, with the exception of contrail cirrus and (direct and indirect) aerosol effects. Furthermore, different future scenarios were employed to analyze

Table 6. Global Annual Mean Surface Temperature Response (mK) for All TRADEOFF Scenarios in 2100 for an Increase of Air Traffic According to the $FA1_{2100}$ Scenario[a]

Scenario	Contrails	H_2O	O_{3S}	CH_4	O_{3L}	CO_2	Total
+2000 ft	9.1 (+0.7)	5.9 (+1.8)	53.4 (+4.4)	−18.9 (+0.2)	−6.3 (+0.1)	53.9 (−0.4)	97.0 (+6.7)
Base case	8.4	4.1	48.9	−19.1	−6.4	54.3	90.3
−2000 ft	7.3 (−1.1)	2.6 (−1.5)	46.0 (−2.9)	−22.5 (−3.4)	−7.5 (−1.1)	55.5 (+1.2)	81.4 (−8.9)
−4000 ft.	5.9 (−2.5)	1.7 (−2.4)	44.7 (−4.2)	−25.8 (−6.7)	−8.7 (−2.3)	56.7 (+2.4)	74.6 (−15.7)
−6000 ft	4.4 (−4.0)	0.9 (−3.2)	42.4 (−6.5)	−27.5 (−8.4)	−9.2 (−2.8)	57.0 (+2.7)	68.0 (−22.3)

[a]Absolute radiative forcing changes relatively to the base case are given in parentheses.

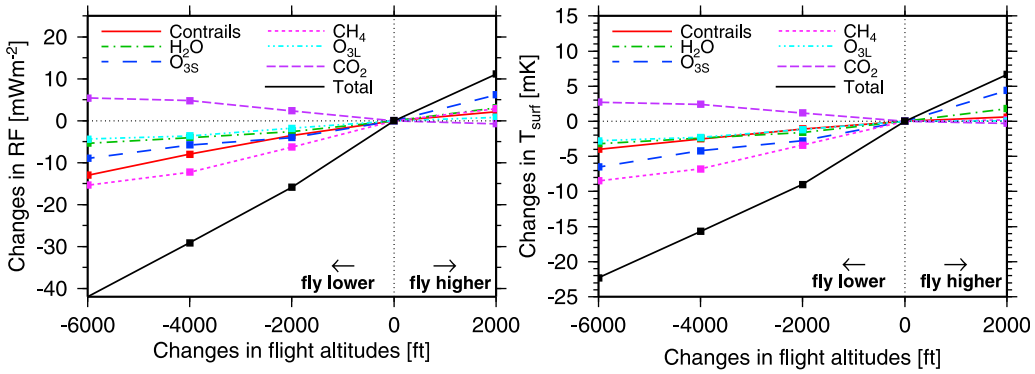

Figure 12. Global annual mean changes of (left) net radiative forcing and (right) surface temperature in 2100 due to CO_2, contrails, H_2O, O_{3S}, CH_4 and O_{3L} for all flight altitude change scenarios relative to the base case for the $FA1_{2100}$ future scenario. The symbols indicate points where data are available, which are connected by straight lines for clarity.

tradeoffs between short and long term effects. On a global annual average, lower flight altitudes yield a reduction of radiative forcing by contrails, ozone, water vapor and methane and a small increase of CO_2 radiative forcing for equilibrium conditions. Higher flight altitudes, in contrast, result in an increase of radiative forcing of ozone, water vapor, contrails and methane and a small decrease of CO_2 radiative forcing. Non-CO_2 effects dominate the comparatively smaller CO_2 effects also for future scenarios with constant or increasing air traffic emissions. However, if air traffic emissions are reduced or even terminated, the radiative forcing of short-lived species will decline quickly but the counteracting CO_2 effect will survive for several centuries. The temperature response follows the radiative forcing development with delay because of the inertia of the climate system. Aviation effects which are not included in this study (such as contrail cirrus and aerosol effects), as discussed in the introduction and results sections, might change the absolute magnitude of radiative forcing and temperature response. The proportion of non-CO_2 effects to CO_2 would change for future scenarios with increasing air traffic and the reversal point when the temperature response changes sign would be shifted in time. The overall result, that short-lived species are reduced for lower flight altitudes and dominate the counteracting CO_2 effect for a future development with increasing air traffic, however, is not expected to change, even if contrail cirrus was included. No information on the altitude sensitivity of indirect aerosol effects is available at present, but if the magnitude of this effect would consolidate near the maximum estimates which are currently discussed [e.g., *Liu et al.*, 2009], a substantial impact on the net effect of flight altitude sensitivity studies cannot be excluded.

[46] The investigated future scenarios make clear, that for any attempt to assess the mitigation of air traffic climate effects, no matter if by operational or other means, the future scenarios must be chosen carefully depending on the mitigation aim, e.g. a fast reduction of climate impacts. Furthermore, the result of the assessment depends crucially on the time horizon of the evaluation of effects i.e. the point in time for which the temperature change is analyzed. Such considerations should be guided by the main objective of the mitigation strategy. Reducing non-CO_2 contributions, which have a short lifetime, at the expense of increased CO_2 emissions, which have a very long lifetime, may yield a favorable environmental effect soon after implementation. However, such a strategy includes the risk of transferring an essential part of the negative effect of increased CO_2 emissions into the far future. The quantitative assessment would

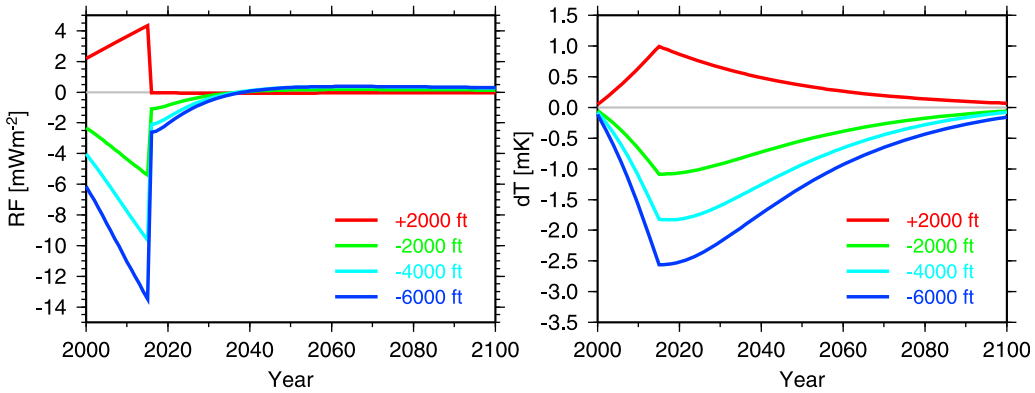

Figure 13. Temporal evolution of the (left) total radiative forcing (mW/m^2) and (right) temperature response changes (mK) arising from changed flight altitudes for the $ZERO_{2015}$ scenario.

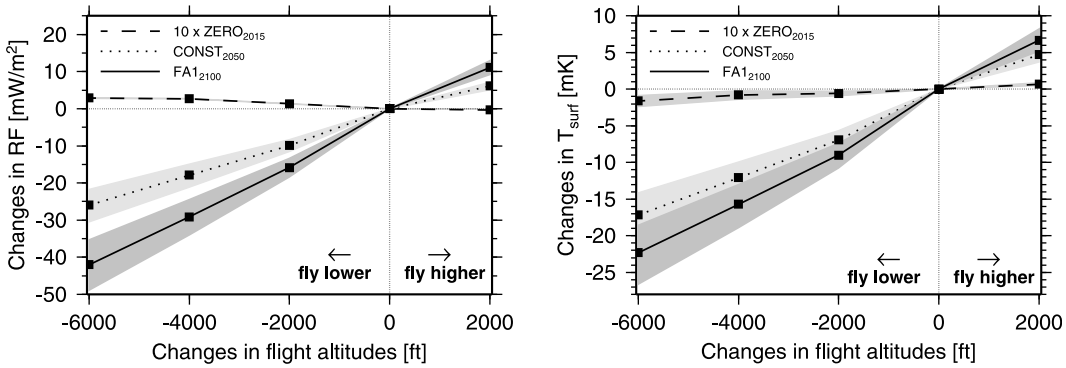

Figure 14. Changes in (left) total net radiative forcing and (right) surface temperature in 2100 for all flight altitude change scenarios relative to the base case for the $ZERO_{2015}$, the $CONST_{2050}$ and the $FA1_{2100}$ future scenario. Note that the values for the $ZERO_{2015}$ scenario were scaled by a factor of 10. Grey shaded areas show the 95% confidence intervals. The symbols indicate points where data are available, which are connected by straight lines for clarity.

depend crucially on the rate of devaluation assumed for long-lived effects, as discussed by *Schwartz Dallara et al.* [2011].

[47] If the mitigation of non-CO_2 aviation effects is attempted by re-routing the actual fleet of aircraft, as discussed within the present study, this would affect the fuel efficiency through different aerodynamics at e.g. different altitudes. A new generation of planes, however, may be designed for minimum fuel consumption at other flight altitudes than today [e.g., *Noppel and Singh*, 2007; *Egelhofer et al.*, 2008; *Koch et al.*, 2011; *Schwartz Dallara et al.*, 2011]. Hence, a fundamental task for reaching optimal mitigation will be the reduction of the climate impact of short-lived species while keeping the counteracting effect of CO_2 at an absolute minimum. This could be achieved e.g. by including the mitigation aspect in the aircraft design process or by reducing speed, as investigated by, e.g., *Schwartz Dallara et al.* [2011].

9. Outlook: Mitigation by Relocating Individual Flights

[48] The present study is based on scenarios that imply a general shift from a standard to an alternative flight altitude and its purpose is to study generalized responses. A relocation of selected individual flight paths (e.g. depending on actual meteorological conditions) cannot be covered with this method. *Mannstein et al.* [2005] proposed that flight altitude changes at the expense of enhanced fuel consumption are worthwhile only for certain ambient conditions, and whether or not flight altitudes are adjusted, should be decided for each flight and each weather situation individually. A general shift of flight altitudes to lower levels will certainly include numerous shifts where no contrails are avoided or no contrails would form anyway or where even additional contrails might form. A strategy that eliminates inefficient flight level changes by individual decision, however, sets much higher demands with respect to a detailed knowledge on ambient conditions and the development of a contrail's life cycle. Including contrail cirrus in the mitigation of individual flights may require detailed forecasts of ice supersaturated regions, contrail lifetime and optical properties, contrail overlap with natural clouds, and atmospheric vertical motion over periods of 10 hours or more [*Minnis et al.*, 1998; *Burkhardt and Kärcher*, 2009]. A step toward this direction is the strategy presented by *Schumann et al.* [2011] who optimize flight routes with respect to minimum total climate impact of contrails and CO_2 depending on the actual meteorological situation by avoiding warming contrails and/or producing cooling contrails through small flight level changes of 2000 ft. However, a mitigation approach based on climatological considerations, as presented in the present study, remains a reasonable option for assessing the mitigation potential and the trade-offs between contrail radiative forcing with additional fuel use and other effects. Furthermore, it may represent a basis for an integrative mitigation solution combining both methods, e.g. choosing a seasonally and regionally optimized standard flight altitude, which can be adapted to the actual weather situation. The overall effect and the potential for mitigation for individual flights' emissions on contrails, ozone, and methane radiative forcing for typical weather situations is investigated within the EU FP7 project REACT4C (http://www.react4c.eu).

[49] **Acknowledgments.** The authors acknowledge funding from the EU FP6 NoE ECATS, the EU FP6 IP QUANTIFY, the EU FP7 project REACT4C and the DLR project CATS. The emission scenarios were established within the EU FP5 project TRADEOFF. D.S.L. was also supported by the UK Department of Transport. The chemistry-climate-model simulations were run on the DKRZ NEC-SX6.

References

Brunner, D., et al. (2003), An evaluation of the performance of chemistry transport models by comparison with research aircraft observations. Part 1: Concepts and overall model performance, *Atmos. Chem. Phys.*, *3*, 1609–1631.

Brunner, D., et al. (2005), An evaluation of the performance of chemistry transport models. Part 2: Detailed comparison with two selected campaigns, *Atmos. Chem. Phys.*, *5*(1), 107–129.

Burkhardt, U., and B. Kärcher (2009), Process-based simulation of contrail cirrus in a global climate model, *J. Geophys. Res.*, *114*, D16201, doi:10.1029/2008JD011491.

Burkhardt, U., and B. Kärcher (2011), Global radiative forcing from contrail cirrus, *Nat. Clim. Change*, *1*(1), 54–58.

Dahlmann, K. (2012), Eine Methode zur effizienten Bewertung von Maßnahmen zur Klimaoptimierung des Luftverkehrs, PhD thesis, Fak. für Phys., Ludwig-Maximilians-Univ. München, Munich, Germany.

Egelhofer, R., C. Marizy, and C. Bickerstaff (2008), On how to consider climate change in aircraft design, *Meteorol. Z.*, *17*(2), 173–179.
Fichter, C. (2009), Climate impact of air traffic emissions in dependency of the emission location and altitude, PhD thesis, Fac. of Sci. and Eng., Manchester Metrop. Univ., Manchester, UK.
Fichter, C., S. Marquart, R. Sausen, and D. Lee (2005), The impact of cruise altitude on contrails and related radiative forcing, *Meteorol. Z.*, *14*(4), 563–572.
Forster, P., M. Ponater, and W. Zhong (2001), Testing broadband radiation schemes for their ability to calculate the radiative forcing and temperature response to stratospheric water vapour and ozone changes, *Meteorol. Z.*, *10*(5), 387–393.
Fouquart, Y., and B. Bonnel (1980), Computations of solar heating of the Earth's atmosphere—A new parameterization, *Beitr. Phys. Atmos.*, *53*, 35–62.
Frömming, C., M. Ponater, U. Burkhardt, A. Stenke, S. Pechtl, and R. Sausen (2011), Sensitivity of contrail coverage and contrail radiative forcing to selected key parameters, *Atmos. Environ.*, *45*, 1483–1490.
Fuglestvedt, J., T. Berntsen, I. Isaksen, H. Mao, X. Liang, and W. Wang (1999), Climatic forcing of nitrogen oxides through changes in tropospheric ozone and methane: Global 3D model studies, *Atmos. Environ.*, *33*(6), 961–977.
Gardner, R., et al. (1997), The ANCAT/EC global inventory of NO_x emissions from aircraft, *Atmos. Environ.*, *31*(12), 1751–1766.
Gauss, M., I. S. A. Isaksen, S. Wong, and W.-C. Wang (2003), Impact of H_2O emissions from cryoplanes and kerosene aircraft on the atmosphere, *J. Geophys. Res.*, *108*(10), 4304, doi:10.1029/2002JD002623.
Gauss, M., I. Isaksen, D. Lee, and O. Søvde (2006), Impact of aircraft NO_x emissions on the atmosphere—Tradeoffs to reduce the impact, *Atmos. Chem. Phys.*, *6*, 1529–1548.
Grewe, V., and A. Stenke (2008), Airclim: An efficient tool for climate evaluation of aircraft technology, *Atmos. Chem. Phys.*, *8*, 4621–4639.
Grewe, V., M. Dameris, R. Hein, I. Köhler, and R. Sausen (1999), Impact of future subsonic aircraft NO_x emissions on the atmospheric composition, *Geophys. Res. Lett.*, *26*(1), 47–50.
Grewe, V., D. Brunner, M. Dameris, J. Grenfell, R. Hein, D. Shindell, and J. Staehelin (2001), Origin and variability of upper tropospheric nitrogen oxides and ozone at northern mid-latitudes, *Atmos. Environ.*, *35*(20), 3421–3433.
Grewe, V., M. Dameris, C. Fichter, and R. Sausen (2002a), Impact of aircraft NO_x emissions. Part 1: Interactively coupled climate-chemistry simulations and sensitivities to climate-chemistry feedback, lightning and model resolution, *Meteorol. Z.*, *11*(3), 177–186.
Grewe, V., M. Dameris, C. Fichter, and D. Lee (2002b), Impact of aircraft NO_x emissions. Part 2: Effects of lowering the flight altitude, *Meteorol. Z.*, *11*(3), 197–205.
Hansen, J., et al. (2005), Efficacy of climate forcings, *J. Geophys. Res.*, *110*, D18104, doi:10.1029/2005JD005776.
Hasselmann, K., R. Sausen, E. Maier-Reimer, and R. Voss (1993), On the cold start problem in transient simulations with coupled atmosphere-ocean models, *Clim. Dyn.*, *9*, 53–61.
Hasselmann, K., S. Hasselmann, R. Giering, V. Ocana, and H. Storch (1997), Sensitivity study of optimal CO_2 emission paths using a simplified Structural Integrated Assessment Model (SIAM), *Clim. Change*, *37*(2), 345–386.
Hein, R., et al. (2001), Results of an interactively coupled atmospheric chemistry-general circulation model: Comparison with observations, *Ann. Geophys.*, *19*(4), 435–457.
Hendricks, J., B. Kärcher, and U. Lohmann (2009), Effects of ice nuclei on cirrus clouds in a global climate model, *J. Geophys. Res.*, *116*, D18206, doi:10.1029/2010JD015302.
Holmes, C., Q. Tang, and M. Prather (2011), Uncertainties in climate assessment for the case of aviation NO, *Proc. Natl. Acad. Sci. U. S. A.*, *108*(27), 10,997–11,002.
Hoor, P., et al. (2009), The impact of traffic emissions on atmospheric ozone and OH: Results from QUANTIFY, *Atmos. Chem. Phys.*, *9*, 3113–3136.
Intergovernmental Panel on Climate Change (2001), *Climate Change 2001: The Scientific Basis. Contribution of Working Group I to the Third Assessment Report of the Intergovernmental Panel on Climate Change*, edited by J. T. Houghton et al., Cambridge Univ. Press, Cambridge, U. K.
International Energy Agency (2007), *Oil Information 2006*, 749 pp., IEA, Paris.
Jacobson, M., J. Wilkerson, A. Naiman, and S. Lele (2011), The effects of aircraft on climate and pollution. Part I: Numerical methods for treating the subgrid evolution of discrete size-and composition-resolved contrails from all commercial flights worldwide, *J. Comput. Phys.*, *230*, 5115–5132.
Kentarchos, A., and G. Roelofs (2002), Impact of aircraft NO_x emissions on tropospheric ozone calculated with a chemistry-general circulation model: Sensitivity to higher hydrocarbon chemistry, *J. Geophys. Res.*, *107*(D13), 4175, doi:10.1029/2001JD000828.
Kingdon, R. (2000), *FAST v1.0 User Manual*, Propul. Dep., DERA Pyestock, Farnborough, U. K.
Koch, A., B. Lührs, K. Dahlmann, F. Linke, V. Grewe, M. Litz, M. Plohr, B. Nagel, V. Gollnick, and U. Schumann (2011), Climate impact assessment of varying cruise flight altitudes applying the CATS simulation approach, paper presented at Third International Conference of the European Aerospace Societies, Venice, Italy.
Köhler, M., G. Rädel, O. Dessens, K. Shine, H. Rogers, O. Wild, and J. Pyle (2008), Impact of perturbations to nitrogen oxide emissions from global aviation, *J. Geophys. Res.*, *113*, D11305, doi:10.1029/2007JD009140.
Lee, D., D. Fahey, P. Forster, P. Newton, R. Wit, L. Lim, B. Owen, and R. Sausen (2009), Aviation and global climate change in the 21st century, *Atmos. Environ.*, *43*, 3520–3537.
Lee, D., et al. (2010), Transport impacts on atmosphere and climate: Aviation, *Atmos. Environ.*, *44*(37), 4678–4734.
Liu, X., J. Penner, and M. Wang (2009), Influence of anthropogenic sulfate and black carbon on upper tropospheric clouds in the NCAR CAM3 model coupled to the IMPACT global aerosol model, *J. Geophys. Res.*, *114*, D03204, doi:10.1029/2008JD010492.
Mannstein, H., P. Spichtinger, and K. Gierens (2005), A note on how to avoid contrail cirrus, *Transport. Res.*, *10*(5), 421–426.
Marquart, S., and B. Mayer (2002), Towards a reliable GCM estimation of contrail radiative forcing, *Geophys. Res. Lett.*, *29*(8), 1179, doi:10.1029/2001GL014075.
Marquart, S., R. Sausen, M. Ponater, and V. Grewe (2001), Estimate of the climate impact of cryoplanes, *Aerosp. Sci. Technol.*, *5*(1), 73–84.
Marquart, S., M. Ponater, F. Mager, and R. Sausen (2003), Future development of contrail cover, optical depth and radiative forcing: Impacts of increasing air traffic and climate change, *J. Clim.*, *16*(17), 2890–2904.
Minnis, P., D. Young, D. Garber, L. Nguyen, W. Smith Jr., and R. Palikonda (1998), Transformation of contrails into cirrus during success, *Geophys. Res. Lett.*, *25*(8), 1157–1160.
Morcrette, J. (1991), Radiation and cloud radiative properties in the European Centre for Medium Range Weather Forecasts forecasting system, *J. Geophys. Res.*, *96*(D5), 9121–9132.
Myhre, G., et al. (2011), Radiative forcing due to changes in ozone and methane caused by the transport sector, *Atmos. Environ.*, *45*(2), 387–394.
Noppel, F., and R. Singh (2007), Overview on contrail and cirrus cloud avoidance technology, *J. Aircraft*, *44*(5), 1721–1726.
Olivié, D., et al. (2012), Modeling the climate impact of road transport, maritime shipping and aviation over the period 1860–2100 with and OAGCM, *Atmos. Chem. Phys.*, *12*, 1449–1480.
Penner, J., et al. (1999), *Aviation and the Global Atmosphere: A Special Report of IPCC Working Groups I and III in Collaboration With the Scientific Assessment Panel to the Montreal Protocol on Substances that Deplete the Ozone Layer*, 373 pp., Cambridge Univ. Press, Cambridge, U. K.
Ponater, M., S. Marquart, and R. Sausen (2002), Contrails in a comprehensive global climate model: Parameterization and radiative forcing results, *J. Geophys. Res.*, *107*(13), 4164, doi:10.1029/2001JD000429.
Ponater, M., V. Grewe, R. Sausen, U. Schumann, S. Pechtl, E. Highwood, and N. Stuber (2006), Climate sensitivity of radiative impacts from transport systems, in *Proceedings of an International Conference on Transport, Atmosphere and Climate (TAC)*, edited by R. Sausen et al., pp. 190–196, Eur. Comm., Luxembourg.
Rädel, G., and K. Shine (2008), Radiative forcing by persistent contrails and its dependence on cruise altitudes, *J. Geophys. Res.*, *113*, D07105, doi:10.1029/2007JD009117.
Rap, A., P. Forster, J. Haywood, A. Jones, and O. Boucher (2010a), Estimating the climate impact of linear contrails using the UK Met Office climate model, *Geophys. Res. Lett.*, *37*, L20703, doi:10.1029/2010GL045161.
Rap, A., P. Forster, A. Jones, O. Boucher, J. Haywood, N. Bellouin, and R. De Leon (2010b), Parameterization of contrails in the UK Met Office Climate Model, *J. Geophys. Res.*, *115*, D10205, doi:10.1029/2009JD012443.
Reithmeier, C., and R. Sausen (2002), ATTILA: Atmospheric tracer transport in a Lagrangian model, *Tellus, Ser. B*, *54*(3), 278–299.
Roeckner, E., K. Arpe, L. Bengtsson, M. Christoph, M. Claussen, L. Dümenil, M. Esch, M. Giorgetta, U. Schlese, and U. Schulzweida (1996), The atmospheric general circulation model ECHAM-4: Model description and simulation of present-day climate, *Rep. 218*, Max-Planck-Inst. für Meteorol., Hamburg, Germany.

Sausen, R., and U. Schumann (2000), Estimates of the climate response to aircraft CO_2 and NO_x emissions scenarios, *Clim. Change*, *44*(1), 27–58.

Sausen, R., K. Gierens, M. Ponater, and U. Schumann (1998), A diagnostic study of the global distribution of contrails. Part I: Present day climate, *Theor. Appl. Climatol.*, *61*(3), 127–141.

Sausen, R., et al. (2005), Aviation radiative forcing in 2000: An update on IPCC (1999), *Meteorol. Z.*, *14*, 555–561.

Schumann, U. (1996), On conditions for contrail formation from aircraft exhausts, *Meteorol. Z.*, *5*, 4–23.

Schumann, U. (2012), A contrail cirrus prediction model, *Geosci. Model Dev.*, *5*, 543–580.

Schumann, U., K. Graf, and H. Mannstein (2011), Potential to reduce the climate impact of aviation by flight level changes, paper presented at 3rd AIAA Atmospheric Space Environments Conference, Am. Inst. of Aeronaut. and Astronaut., New York.

Schwartz Dallara, E., I. Kroo, and I. Waitz (2011), Metric for comparing lifetime average climate impact of aircraft, *AIAA J.*, *49*(8), 1600–1613.

Steil, B., M. Dameris, C. Brühl, P. Crutzen, V. Grewe, M. Ponater, and R. Sausen (1998), Development of a chemistry module for GCMs: First results of a multiannual integration, *Ann. Geophys.*, *16*(2), 205–228.

Stenke, A., V. Grewe, and M. Ponater (2008), Lagrangian transport of water vapor and cloud water in the ECHAM4 GCM and its impact on the cold bias, *Clim. Dyn.*, *31*(5), 491–506.

Stenke, A., M. Dameris, V. Grewe, and H. Garny (2009), Implications of Lagrangian transport for simulations with a coupled chemistry-climate model, *Atmos. Chem. Phys.*, *9*, 5489–5504.

Stevenson, D., R. Doherty, M. Sanderson, W. Collins, C. Johnson, and R. Derwent (2004), Radiative forcing from aircraft NO_x emissions: Mechanisms and seasonal dependence, *J. Geophys. Res.*, *109*, D17307, doi:10.1029/2004JD004759.

Stordal, F., et al. (2006), TRADEOFFs in climate effects through aircraft routing: Forcing due to radiatively active gases, *Atmos. Chem. Phys. Discuss.*, *6*, 10,733–10,771.

Stuber, N., and P. Forster (2007), The impact of diurnal variations of air traffic on contrail radiative forcing, *Atmos. Chem. Phys.*, *7*, 3153–3162.

Stuber, N., R. Sausen, and M. Ponater (2001), Stratosphere adjusted radiative forcing calculations in a comprehensive climate model, *Theor. Appl. Climatol.*, *68*(3), 125–135.

Unger, N. (2011), Global climate impact of civil aviation for standard and desulfurized jet fuel, *Geophys. Res. Lett.*, *38*, L20803, doi:10.1029/2011GL049289.

Wild, O., M. Prather, and H. Akimoto (2001), Indirect long-term global radiative cooling from NO_x emissions, *Geophys. Res. Lett.*, *28*(9), 1719–1722.

Wilkerson, J., M. Jacobson, A. Malwitz, S. Balasubramanian, R. Wayson, G. Fleming, A. Naiman, and S. Lele (2010), Analysis of emission data from global commercial aviation: 2004 and 2006, *Atmos. Chem. Phys.*, *10*, 6391–6408.

Williams, V., R. Noland, and R. Toumi (2002), Reducing the climate change impacts of aviation by restricting cruise altitudes, *Transport. Res.*, *7*(6), 451–464.

Williamson, D., and P. Rasch (1994), Water vapor transport in the NCAR CCM2, *Tellus, Ser. A*, *46*(1), 34–51.